Nanophase segregation of nonpolar solvents in smectic liquid crystals of bent-shape molecules

M. Y. M. Huang,[1] A. M. Pedreira,[2] O. G. Martins,[2] A. M. Figueiredo Neto,[2] and A. Jákli[1]
[1]*Liquid Crystal Institute, Kent State University, Kent, Ohio 44242*
[2]*Instituto de Física, Universidade de São Paulo, Caixa Postal 66318, 05315-970, São Paulo, SP, Brazil*
(Received 21 February 2002; published 24 September 2002)

Electro-optical, calorimetric, x-ray, and dielectric measurements are reported on a mixture containing a bent-core liquid crystal 4-chloro-1,3-phenylinebis [4-(4-*n*-tetradecyloxyphenyliminomethyl) benzoate] mixed with the nonpolar solvent *n*-hexadecane (HEX). It is observed that the addition of HEX depresses the isotropic-to-smectic phase transition temperature, but the crystallization temperature does not change considerably. Instead, the texture of the crystalline phase changes and, at sufficiently high concentrations of HEX (>20 wt %), an optically isotropic phase appears. Above 40 wt % HEX concentrations, the mesophase completely disappears and a direct isotropic solid-to-isotropic liquid transition takes place. At increasing HEX concentration, the transition enthalpies, the layer ordering, and the magnitude of the electric polarization decrease. X-ray studies reveal that HEX molecules pack in between the smectic layers, resulting in an increase of the layer spacing by about 3 Å. The increase of the layer spacing saturates at 5 wt % of HEX. The phase segregation observed seems to be due to steric interactions between the flexible HEX molecules and the rigid bent cores of the liquid crystal molecules.

DOI: 10.1103/PhysRevE.66.031708 PACS number(s): 61.30.Eb, 61.30.Cz, 61.30.Gd

I. INTRODUCTION

Recently, it was shown that dissolving a thermotropic liquid crystal composed by polar disc-shaped molecules into nonpolar organic solvents [1] could produce ferroelectric liquid crystals with remarkable properties. It turned out that the electro-optical switching properties of the solutions are, to some extent, better than those of the pure columnar liquid crystals, since the switching threshold and the phase transition temperatures are lowered [2]. These results imply that thermotropic mesophases in nonaqueous solvents can be used in electro-optical devices, and motivated us to explore similar mixtures with polar ''banana-shaped'' molecules [3,4]. Although this type of mixture was named lyotropic [1], it seems to be more appropriate to refer to it simply as a mixture since one of its initial compounds already has mesophases. The term ''swollen thermotropic'' is also not applicable to this system since the solvent induces new liquid crystalline phases that are not present in the pure thermotropic liquid crystal.

Previous studies on a ferroelectric ''banana-smectic'' material mixed with nonpolar xylene showed [5] that the solvent drastically widens the ferroelectric electro-optical switching range and lowers the clearing point. For both steric and chemical reasons, the xylene molecules are supposed to sit between the rigid cores of the banana-shaped molecules, thus weakening the dipole-dipole interactions. However, it is known that there is a tendency for segregation of rigid and flexible (furthermore linear and bent) molecular segments in such a way that similar segments pack together. Accordingly, flexible nonpolar alkyl chains should prefer to pack together with the aliphatic chains [6], and would avoid contact with the rigid bent core of the liquid crystal molecules.

The addition of organic solvents to host thermotropic (calamitic) smectic liquid crystals shows that the layer spacing increases with increasing amounts of solvent [7]. Moreover, the experimental x-ray diffraction results point toward a nanosegregation effect with the solvent molecules concentrating themselves (principally) in between the smectic layers.

In this paper, we report studies on a bent-core molecule dissolved in *n*-hexadecane [CH_3-(CH_2)14-CH_3] at different concentrations, which should impose both flexible and steric forces on the liquid crystal molecules. X-ray diffraction, scanning calorimetric, and dielectric techniques are used to investigate the physical-chemical properties of these mixtures.

II. EXPERIMENT

A. Materials

The bent-core liquid crystalline molecule used is 4-chloro-1,3-phenylinebis [4-(4-*n*-tetradecyloxyphenyliminomethyl)benzoate] [8], (C14 for short). It was synthesized in the Stranski Laboratory of the Technical University of Berlin and provided for us by Dr. H. Sawade and Professor G. Heppke. The phase sequence of this material observed as a function of the temperature is

$$\mathrm{Cry} \xrightarrow[68\,^\circ\mathrm{C}]{} \mathrm{Sm}CP \xrightarrow[127\,^\circ\mathrm{C}]{} \mathrm{ISO},$$

where Cry, SmCP, and ISO stand for the crystalline, polar smectic-C, and isotropic phases, respectively. At lower temperatures the stable state is crystalline, but, on cooling from the SmCP phase, a metastable state (SmX) is observable below 60 °C. Figure 1 shows the molecular structure of the

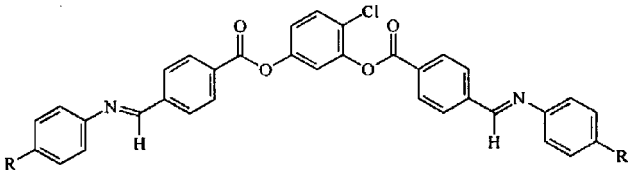

FIG. 1. Molecular structure of the 4-chloro-1,3-phenylinebis [4-(4-*n*-tetradecyloxyphenyliminomethyl)benzoate].

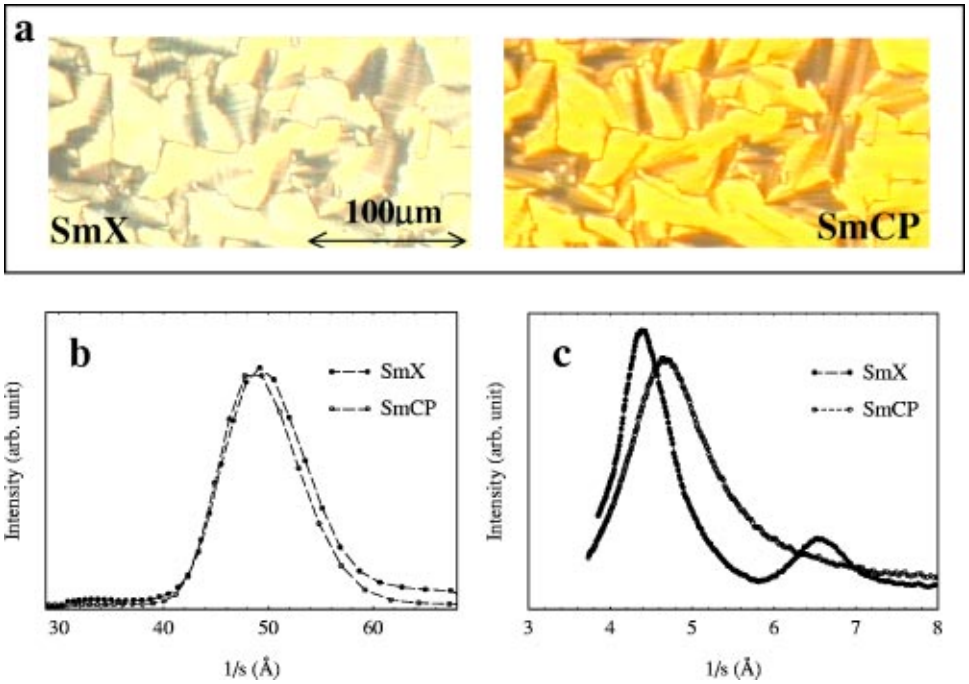

FIG. 2. Textures (a) and x-ray diffraction profiles of the pure liquid crystal C14 in small angles (b) and high angles (c). The pictures show textures of 4 μm films between crossed polarizers at 80 °C (Sm*CP* phase) and at 24 °C (metastable Sm*X* phase). The corresponding x-ray profiles are obtained on powder samples. $s = 2 \sin \theta/\lambda_x$, where 2θ is the scattering angle [10].

C14.

The *n*-hexadecane (HEX) is from Merck (boiling point: 287 °C, density: $\rho = 0.77$ g/cm^3, purity: better than 99.5%) [9]. Mixtures were prepared by mixing the compounds at temperature $T \sim 130$ °C, with the C14 in the ISO phase, and afterwards placed in different sample holders used in each experimental setup.

B. Setups

1. X-ray diffraction setup

Lindemann glass capillaries of 1.0 mm diameter were filled with the samples at different HEX concentrations and placed in a temperature controlled device (accuracy of 0.5 °C). The sample holder was placed in an x-ray generator (Rigaku) with a monochromatic beam (graphite monochromator, $\lambda_x = 1.54 \times 10^{-1}$ nm) in a Laue-type scattering geometry [10] with a pinhole collimator of 0.5 mm diameter. The diffraction patterns were registered in imaging plates, digitized, and analyzed by a PC. The experiments were done with nonoriented samples (powder-type exposures).

2. Differential scanning calorimeter (DSC) setup

Calorimetric measurements were carried out using a Perkin Elmer DSC7, placing the materials in 30 μl pans. The

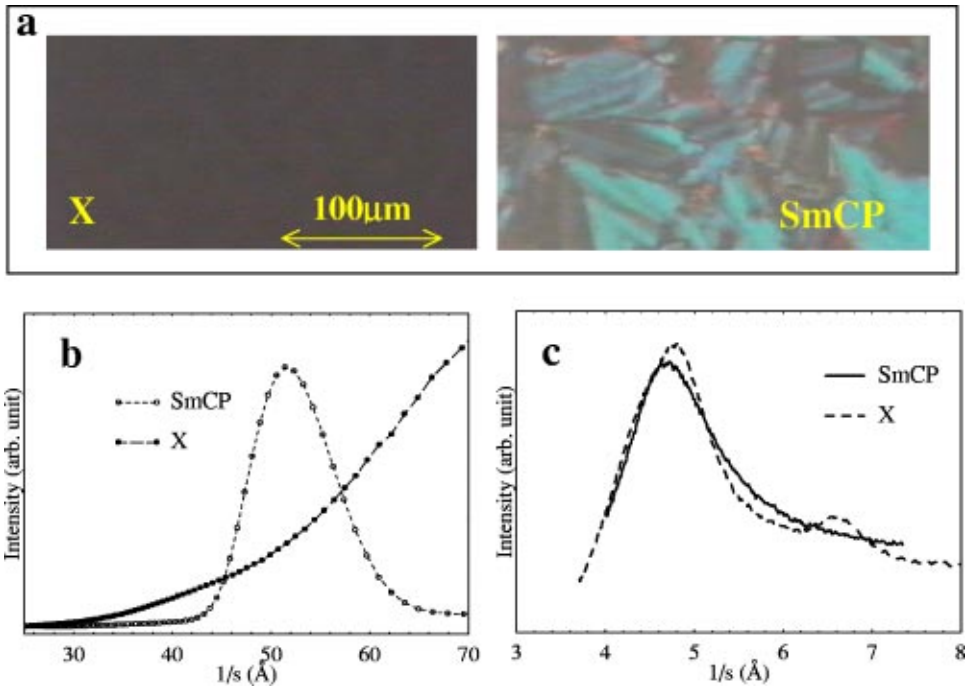

FIG. 3. Textures (a) and x-ray profiles in small angles (b) and high angles (c) of the Sm*CP* phase and unknown *X* phase for the 40 wt. % HEX-C14 system at 68 °C and 24 °C, respectively.

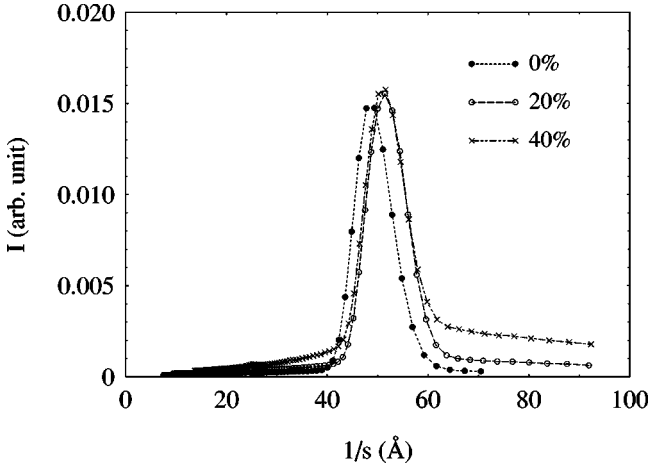

FIG. 4. First-order Bragg scattering peak profiles from the smectic layers. Samples with different concentrations of HEX: at 80 °C (0 wt. %), at 79 °C (20 wt. %), and at 68 °C (40 wt. %).

measurements were carried out at 3 °C/min cooling-heating rates.

3. Dielectric measurements setup

Dielectric measurements were carried out by a Quadtech 1920 Precision LCR meter between 20Hz and 1MHz in ready-made 4 μm thick cells purchased from Displaytech with uniform planar alignment coatings. The temperature was regulated with an accuracy of 0.5 °C by placing the sample in an Instec hot stage HS1.

4. Electro-optical measurements setup

The materials were filled in 4 μm Displaytech cells. The liquid crystal cells were placed in a computer controlled hot stage (STC200F from Instec) and the phase sequences were investigated by polarizing microscopy (BX60 from Olympus). Electric current (polarization) measurements and electro-optical studies were carried out in the entire Sm*CP* ranges in 1 K steps. For these measurements, a digital oscilloscope (HP 54600B), a digital multimeter (HP 34401A), and an arbitrary waveform generator (HP 33120A) were used.

III. RESULTS AND REMARKS

The x-ray profile and the microscopic texture of the pure C14 are shown in Fig. 2. Peaks at small angles show layer spacings of 48.5 Å and 49.5 Å in the Sm*CP* and Sm*X* phases, respectively. The high-angle peaks indicate fluidlike in-layer structures with intermolecular distances of 4.7 Å (Sm*CP*) and 4.4 Å (Sm*X*). Although the texture of the metastable Sm*X* state is very similar to the Sm*CP* phase, the x-ray profiles show additional periodicities in both small and high angles (33.2 Å and 6.6 Å, respectively), indicating some kind of frustration in the structure.

When HEX is mixed with C14 the clearing point is suppressed considerably (e.g., to 91 °C at 27 wt. % and to 77 °C at 40 wt. % HEX concentrations, where wt. % stands for weight percent). This trend is similar to previous results on

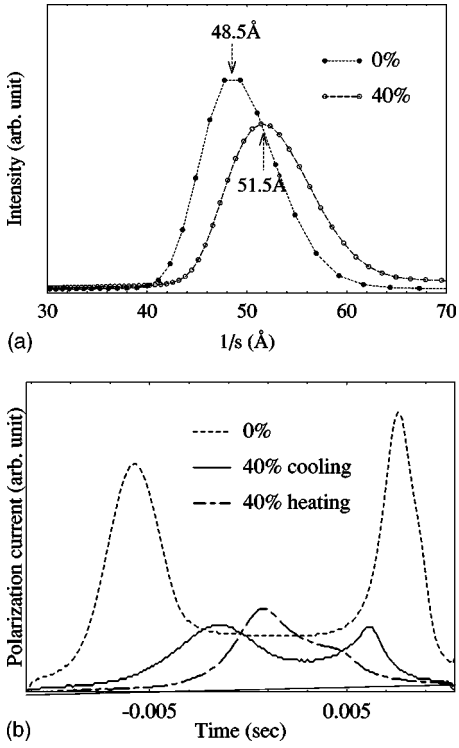

FIG. 5. Comparison of the Sm*CP* structures for the pure C14 at 80 °C and for the 40 wt. % *n*-hexadecane mixtures at 68 °C. (a) Small-angle x-ray scattering peak profiles indicating layer spacing of 48.5 Å and 51.5 Å at 0 wt. % and 40 wt. % HEX concentrations, respectively. (b) Polarization currents as a function of the time. Pure C14 at 80 °C and 40 wt. % HEX system at 68 °C on cooling and heating processes.

xylene molecules [5], but here the switchable range does not extend with increasing solvent concentration, and nonswitchable metastable states appear close to the temperature where Sm*X* is formed in the pure C14. The textures and the corresponding x-ray profiles of the mixture with 40 wt. % of HEX are shown in Fig. 3. With increasing HEX concentration, the textures of the metastable states gradually lose the features of the Sm*CP* phase and become optically isotropic above 20 wt. % HEX concentrations. We label this state hereafter by *X*.

The small-angle x-ray profiles (Fig. 4) show that the layer spacing in the 40 wt. % of HEX mixture is about 3 Å larger than that in the pure C14. Moreover, the width at half height of the small-angle scattering peaks increases at larger HEX concentrations, indicating a decrease of the interlayer ordering (Fig. 4). These features are shown separately in Fig. 5(a), as well. It can be seen that the peaks become wider, especially noticeable in the tail at larger distances. In the metastable *X* state the difference is even greater: only the small-angle scattering is present [Fig. 3(b)], indicating the absence of long-range positional correlation ordering typical of the smectic structure. The high-angle x-ray profiles are very similar to the pure C14, i.e., they show relatively wide peaks at 4.7 Å (Sm*CP*), 4.8 Å, and 6.6 Å (*X* phase).

Differential scanning calorimeter data obtained for a series of mixtures of C14 and HEX show that the transition enthalpies are strongly decreasing with increasing concentra-

TABLE I. Transition temperatures and enthalpies of the mixtures as a function of the HEX concentration (in wt. %) in the range from the pure C14 up to 40 wt. % of HEX.

HEX (wt. %)	Transition temperature (°C) and enthalpy (J/g) (in brackets)			
	Heating (3 °C/min)		Cooling (3 °C/min)	
	X-Sm*CP*	Sm*CP*-ISO	ISO-Sm*CP*	Sm*CP*-X
0	68 (27)	127 (17)	125 (16)	62 (20)
14	69 (14)	107 (3)	107 (3.1)	69 (9.5)
20	73 (10.5)	98 (2.5)	99 (2.7)	67 (8.3)
27	72 (9.5)	88 (2)	91 (2.2)	70 (7.3)
40	71 (5.4)	74 (1.1)	77 (1.2)	66 (6.4)

tions. This is understandable since the layer ordering is decreasing with increasing HEX concentration. Table I shows the transition temperatures and the enthalpies of mixtures with increasing concentrations from the pure C14 up to 40 wt. % of HEX. Above 45–50 wt. % of HEX, the Sm*CP* range disappears and there is a direct transition between two optically isotropic states (ISO and the *X* phase). The transition temperatures and the enthalpies on cooling and heating at larger than 40 wt. % HEX concentrations are presented in Table II. We have to emphasize that at these high HEX concentrations, the phase transitions are wide (especially on cooling), probably due to a phase separation process. Accordingly, the determined transition enthalpies are only approximate.

The electro-optical behavior of the mixtures in films of a few microns thickness can be summarized as follows.

(a) In mixtures of larger than 10 wt. % HEX concentrations, smooth nematiclike textures form on cooling from the isotropic phase. Those samples have large apparent conductivities (10^{-6}–10^{-7} Ωm^{-1}) and show only weak electro-optical response.

(b) On applying a strong field (~ 4 V/μm), the conductivity drops by more than two orders of magnitude and the texture responds as the Sm*CP* phase in the chiral state. This response and the switching angles (twice the director tilt) are similar to that of the pure material except that the threshold for the antiferroelectric to ferroelectric transition is smaller.

(c) The apparent polarization (P_s) involved in the switching decreases strongly with increasing HEX concentration (e.g., at 5 °C below the clearing points, $P_s \sim 480$ nC/cm^2 for the pure C14, $P_s \sim 200$ nC/cm^2 for the 27 wt. % HEX concentration, and $P_s \sim 140$ nC/cm^2 for the 40 wt. % HEX concentration). The reduction of the polarization is about twice as large as would be expected just taking into account the dilution effects. This indicates that the dipole-dipole interactions are suppressed by the presence of the solvent.

(d) At increasing HEX concentrations the switching becomes more and more ferroelectriclike. It is especially pronounced on heating from the lower temperature phase. It is illustrated in Fig. 5(b), where the polarization curves were plotted for the pure C14 and for the 40 wt. % HEX concentration both in cooling and heating.

The dielectric observations can be summarized as follows.

(a) At low temperatures (below 60 °C) relaxations are above 1 MHz for the 10 wt. % of HEX, at around 0.9 MHz for the 20 wt. % of HEX, and at 0.4 MHz for both the metastable state of the pure C14 and the optically isotropic 40 wt. % HEX mixture. The matching of the relaxation frequencies in the pure C14 and the 40 wt. % HEX mixture might indicate that, in this mixture, most of the HEX is separated out from the C14 domains. Figure 6 shows the frequency dependence of the imaginary part of the complex dielectric constant (ε'') for different HEX concentrations.

(b) At high temperatures (above 65 °C) there are relaxations at $f_r \sim 10$ kHz for the pure C14. The relaxation frequency decreases with increasing HEX concentrations (Fig. 7). For example, at 70 °C, $f_r(0\ \text{wt.}\%) = 9\,070$ Hz, $f_r(10\ \text{wt.}\%) = 6\,820$ Hz, $f_r(20\ \text{wt.}\%) = 6\,470$ Hz, and $f_r(40\ \text{wt.}\%) = 3\,980$ Hz. The temperature dependencies of the relaxation frequencies (as determined from the maxima of the dielectric loss ε'') are plotted in Fig. 8.

The activation energies determined by the slopes of the temperature dependence of the relaxation frequencies, assuming an Arrhenius behavior, are presented in Table III and

TABLE II. Transition temperatures and enthalpies of the mixtures as a function of the HEX concentration in the range from 55 wt. % until 84 wt. % of HEX.

HEX (wt. %)	Transition temperature (°C) and enthalpy (J/g) (in brackets)	
	Heating (3 °C/min)	Cooling (3 °C/min)
	X-ISO	ISO-X
55	68–74(6)	62–66(5)
70	74(15)	65–70(8)
84	75(14)	65–70(12)

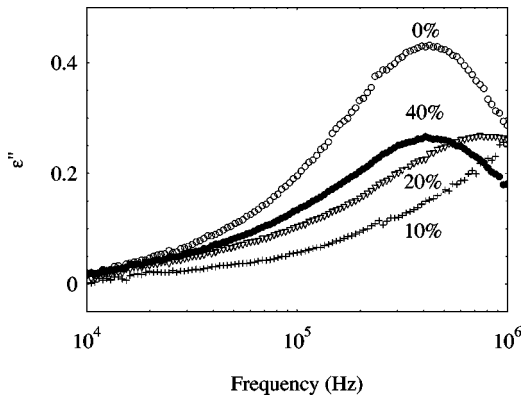

FIG. 6. Frequency dependencies of the imaginary part of the complex dielectric constant for different concentrations of HEX at 24 °C.

Fig. 8. As expected, the activation energies in the ISO phase decrease with increasing HEX concentrations. However, in the Sm*CP* phase the activation energies increase with increasing HEX concentrations, which indicates the appearance of an additional in-plane order. This is in accordance with the additional high-angle peak observed by x ray [see Fig. 3(c)]. The low temperature phases (*X* and Sm*X*) show negative slopes, indicating that they are metastable.

IV. DISCUSSION

Our experimental results show that the HEX molecules form a nanostructure set by the periodicity of the smectic layers. We have to note that nanophase segregation effects were already reported in other smectic systems as well. In the first example [7], organic solvents, similar to those in our studies, were dissolved in chiral rod-shaped molecules possessing nematic and Sm*C** phases. The observed increase of the layer spacing was comparable to our results, with the difference that, there, even higher solvent concentrations could be used. The second example is the observation of layer spacing increase in azo dye-doped smectic liquid crystals due to photo-induced *trans*-to-*cis* photoisomerization [11]. In this latter case the increment of the layer spacing was

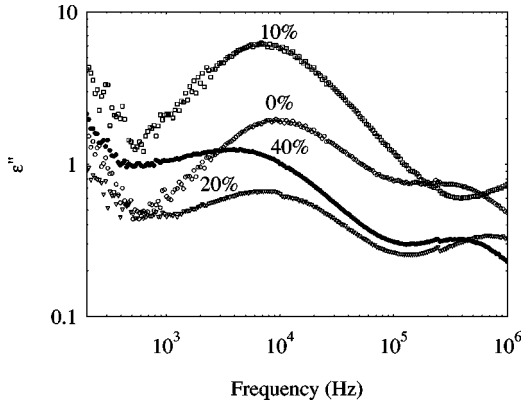

FIG. 7. Frequency dependencies of the imaginary part of the complex dielectric constant for different concentrations of HEX at 70 °C (Sm*CP* phase).

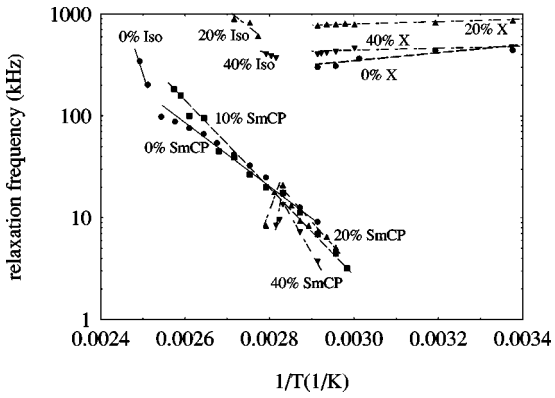

FIG. 8. Relaxation frequencies as a function of the inverse temperature. The lines correspond to fits assuming Arrhenius behavior.

only a small fraction of the increment observed here. Basically, both in the calamitic smectics and in our banana smectics, the steric interaction is the driving mechanism for the nanophase segregation. In the dye-doped system the bent *cis* conformation of the dye molecules and the rod-shaped liquid crystal molecules are incompatible, whereas in the case of organic solvents the rigid cores of the liquid crystal molecules are incompatible with the flexible aliphatic molecules. We observed that the increase of the interlayer spacing distance saturates at 6% of its value in the pure C14 Sm*CP* phase. Assuming that, at low concentrations, all the HEX molecules sit between the layers, and taking into account that the density of the HEX is about $\frac{3}{4}$ of the C14 density, we conclude that the HEX molecules can accommodate uniformly between the layers only up to 5 wt. % of HEX. At higher concentrations the distribution of the layer spacing becomes nonuniform, which in the x-ray profile shows up as wider small-angle peaks (see Figs. 2 and 4). In the lower temperature range both the Sm*X* and *X* states show an additional periodicity of 6.6 Å in the high-angle x-ray profiles. This indicates that the metastable smectic domains have intralayer ordering. In connection with the appearance of the intralayer ordering, the *n*-hexadecane molecules are pushed into the layers. The steric incompatibility between the flexible linear solvent and the rigid bent cores of the C14 molecules would push the HEX molecules to regions with lower concentrations of C14, leading to a submicrometer segregation of the solvent. This result is corroborated by x-ray dif-

TABLE III. Activation energies in units of 10^{-20}J as determined by the slopes of the temperature dependence of the relaxation frequencies, assuming an Arrhenius behavior, and using the data presented in Fig. 8.

Phase / wt. % of HEX	ISO	Sm*CP*	X
0 wt. %	4.2	1	−0.13
10 wt. %		1.3	
20 wt. %	1.1	1.5	−0.05
40 wt. %	0.8	2.0	−0.05

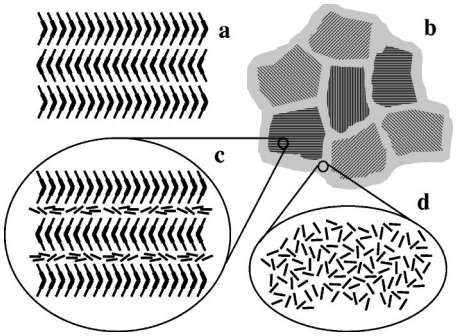

FIG. 9. Structural model for the packing of the molecules for the pure banana-shaped liquid crystal and for the mixture containing *n*-hexadecane. (a) Antiferroelectric molecular packing of the pure C14 (the tilt of the molecular planes is not indicated). (b) Submicrometer-segregated isotropic HEX domains surrounding the smectic domains of C14 with the layered nanosegregated HEX molecules. (c) Magnified local structure of the smectic domains with the nanosegregated HEX molecules. (d) Magnified local structure of the submicrometer-segregated HEX molecules.

fraction experiments. At high angles, the diffraction patterns show that the intermolecular distances inside the layers decrease from 4.6 Å in the pure C14 (temperature of 80 °C) to 4.3 Å in the mixture with 20 wt. % HEX (temperature of 79 °C) and return to 4.7 Å in the mixture with 40 wt. % of HEX (temperature of 68 °C). At small angles [Fig. 3(b)] no interference peak is observed, which is typical for noncorrelated scattering centers of nanometric dimensions. At increasing HEX concentrations the size of the separated HEX domains increase and the correlation between the smectic domains decrease. Due to the isotropic nature of the solvent at sufficiently high concentrations (about 20 wt. % of HEX), the alignment of the smectic domains becomes uncorrelated and the texture becomes optically isotropic. The optical uniformity of this state, observed in the polarizing light microscope, indicates that the sizes of the segregated domains are in the submicrometer range. The structural model based on the x-ray scattering observations is depicted in Fig. 9. At larger than 50 wt. % of HEX concentrations, the size of the separated domains is in the micrometer range, which can be seen in an optical microscope and by the DSC data.

Nanophase segregation of nonpolar molecules in polar liquid crystal media should have a broad range of application in nanotechnology.

ACKNOWLEDGMENTS

This work was supported by the NSF through ALCOM Grant No. DMR 89-20147, and by Brazilian research agencies FAPESP, PRONEX, and CNPQ. We are grateful to Dr. H. Sawade and Professor G. Heppke for providing the liquid crystal for us.

[1] N. Usol'tseva, K. Praefcke, D. Singer, and B. Gündogan, Liq. Cryst. **16**, 601 (1994).
[2] G. Heppke, D. Krüerke, M. Müller, and H. Bock, Ferroelectrics **179**, 203 (1996); D. Krüerke, P. Rudquist, S.T. Lagerwall, H. Sawade, and G. Heppke, *ibid.* **243**, 207 (2000).
[3] Y. Matsunaga and S. Miyamoto, Mol. Cryst. Liq. Cryst. **237**, 311 (1993); H. Matsuzaki and Y. Matsunaga, Liq. Cryst. **14**, 105 (1993).
[4] T. Niori, T. Sekine, J. Watanabe, T. Furukawa, and H. Takezoe, J. Mater. Chem. **6**, 1231 (1996).
[5] A. Jákli, W. Cao, Y. Huang, C.K. Lee, and L-C. Chien, Liq. Cryst. **28**, 1279 (2001).
[6] F. Dowell, Phys. Rev. A **28**, 3520 (1983).
[7] T.P. Rieker, Liq. Cryst. **19**, 497 (1995).
[8] W. Weissflog, C. Lischka, S. Diele, G. Pelzl, and I. Wirth, Mol. Cryst. Liq. Cryst. **328**, 101 (1999).
[9] D.R. Link, G. Natale, R. Shao, J.E. Maclennan, N.A. Clark, E. Körblova, and D.M. Walba, Science **278**, 1924 (1997).
[10] L.V. Azároff, *Elements of X-Ray Crystallography* (McGraw-Hill, New York, 1968).
[11] Y. Lansac, M.A. Glaser, N.A. Clark, and O. Lavrentovich, Nature (London) **398**, 54 (1999); S.K. Prasad and G.G. Nair, Adv. Mater. **13**, 40 (2000); see also A.M. Levelut and M. Clerk, Liq. Cryst. **24**, 105 (1998), and references therein.